Journal of Mechanical Engineering and Sciences
ISSN (Print): 2289-4659; e-ISSN: 2231-8380
Volume 13, Issue 4, pp. 5988-6006, December 2019

DOI: https://doi.org/10.15282/jmes.13.4.2019.18.0474

An integrated experimental and numerical method to assess the fatigue performance of recycled rail

Y. L. Fan[1], N. Perera[2*] and K. Tan[3]

[1] Department of Mechanical Engineering, Sungkyunkwan University,
Suwon, Gyeonggi-do, 16419, Korea
[2] School of Engineering and the Built Environment,
Faculty of Computing, Engineering and the Built Environment,
Birmingham City University, Birmingham, B4 7XG, UK
[*]Email: noel.perera@bcu.ac.uk
Phone: +4401213315745
[3] Department of Mechanical and Construction Engineering,
Faculty of Engineering and Environment, Northumbria University,
Newcastle upon Tyne, NE1 8ST, UK

ABSTRACT

Recycling of rail is practised in the railway industry to promote sustainability and economic efficiency. The functional reliability of recycled rail has to be addressed to ensure safe application. Studies on the reliability of railway rails place great emphasis on fatigue failure. However, scarcity of public domain data on recycled rails and limitation of experimental hardware capability has constrained the study on the fatigue of recycled rails. The aim of the investigation is to propose a novel integrated approach for exploring the fatigue performance of recycled rail effectively and efficiently. A high cycle fatigue test was conducted on a recycled rail specimen to obtain data for the validation of the finite element (FE) numerical model. Following this, the FE numerical model was incorporated with the stepwise load increase test (LIT) method. The integrated method gave a more conservative prediction of the fatigue performance than the analytical method. The shot blasting process induced compressive residual stress which affected the specimen's fatigue performance. This result was demonstrated by the integrated method. Furthermore, this integrated method also successfully reduced the overall required test time. The predicted endurance limit of the specimen was 130.37MPa, accomplishing the BS EN 13674-1:2011 standard.

Keywords: Recycled rail; large scale system; fatigue testing; stepwise load increase test method.

INTRODUCTION

Recycling of rail has been practised in the railway industry to promote sustainability and economic efficiency. One of the methods of recycling is to refurbish the old rails and cascade them to secondary lines with lower traffic density [1]. The rail refurbishment process begins with an on-site inspection to determine suitability to reuse. Qualified rails will then be cut into shorter sections of 18m. Then, the old rails undergo shot blasting surface treatment. The

rails are then realigned by rolling and pressing processes, re-profiled and put under ultrasonic inspection before flash-butt welded to form rails length up to 108m. In the UK, recycled rail make up 8-10% of the rail required in a year [2]. Recycled rails cost 70% less than new rails [2] and the industry records a saving of approximately £4 million per annum [3]. Despite the benefits, the functional reliability of recycled rail has to be addressed to ensure that it is safe to be reused in secondary railway lines.

Studies on the reliability of railway rails place great emphasis on fatigue failure and surface damage due to the characteristic of loadings on rails. BS EN 13674-1:2011 [4] verifies that one of the tests for rail steel is high cycle fatigue testing. The recycled rail should meet the fatigue test qualifying criteria for it to be suitable for reuse. However, there are limited published literature on the material properties, mechanical properties and fatigue testing of recycled rail.

Fatigue is a phenomenon that causes a material to crack or fracture gradually when subjected to cyclic stress and strain. For rail tracks, repeated wheel-rail contact and interaction contribute to fatigue failure. Successive compressive and rolling contact loadings cause plastic deformation of the rails. This promotes the initiation of surface or subsurface cracks and their propagation due to the unidirectional accumulation of strain that propagates downwards [5]. Shot blasting is the key process that restores the strength of old rails. It is a cold treatment process that bombards the metallic surface with minute and firm particles at a high velocity to alter the component's surface condition. It removes the rust to repair the surface and strengthen the metal. Shot blasting causes the plastic deformation and the development of residual stresses of a few hundredths of a millimetre thick on the material surface. The advantage of this process is that it can enhance the mechanical characteristics of the rails by raising its resistance to fatigue and corrosion [6].

Fatigue performance of aluminium after undergoing shot blasting [7] and various other steels [8-12] have been widely published. These shot blasted metallic components have been experimentally tested by exposing them to constant [8, 9] or variable amplitude loading [10], low cycle and high cycle [11] or bending fatigue tests [7]. Respective fatigue performances were obtained and the generated outcomes were positive including significant improvements despite the existence of the stress concentrations [7]. Shot blasting was the main contributing factor to the enhanced fatigue performance by inducing the compressive residual stress to the surface layer of the material [8]. This induced stress, assisted in slowing the crack initiation therefore reducing the rate of the crack propagation. The stability of the residual stress significantly contributes to the beneficial effects of the compressive residual stress [8]. When the total external applied stress and compressive residual stress exceeds the yield strength of the material, the compressive residual stress will decrease. Precedent work on other shot blasted metals under different types of loadings highlighted a positive extension to its usage life.

Fatigue analysis can be interpreted based on the stress-life method, strain-life method or fracture mechanism approach. As recommended by BS EN 13674-1:2011 [4], the test for rail steel is a constant amplitude stress-controlled fatigue test such as the Wöhler's method. This test method is a stress-life approach that utilises the simple or nominal engineering stress to measure the fatigue performance. Data obtained from the stress-controlled fatigue tests are plotted as the nominal stress amplitude (S) against the number of cycles to failure (N), forming an empirical S-N curve. For regular metals such as steel, it is possible to predict the S-N fatigue characteristic analytically using Basquin's equation (Eq. (1)). This is due to the

availability of reliable data in the public domain which were obtained from the numerous experimental tests that were performed.

$$S = aN^b \quad (1)$$

where S = Stress amplitude; a, b = Empirical constants; N = Number of cycles

However, Wöhler's method being statistical in nature requires numerous specimens and test runs generally to failure to generate consistent and reliable results. It induces high material cost and is time consuming. High strength materials like rail steel with long life fatigue will require ultrasonic fatigue test equipment to attain the desired high frequency and fatigue results within reasonable testing time [13].

The stepwise load increase test (LIT) is the single accelerated fatigue characterisation time efficient test method test [14] which is an alternative to the Wöhler's method. It has been utilised for composite materials [14,15] and metals [16-18] and has demonstrated the ability to provide a consistent approximation of a material's endurance limit [15,16]. The stepwise LIT method utilises the continuous amplitude of load/stress divided by the number of cycles (load step) [19]. Providing that the component does not fail, the amplitude of load/stress is increased at regular intervals without changing any other parameters for the next load step. This process is continued till component failure is achieved to identify its fatigue limit. This stepwise load increase test (LIT) technique can be coupled with other suitable measuring techniques to determine a material's endurance limit. Measurement methods such as measuring the strain amplitude [15] or voltage and/or temperature [14,16,17] are some of methods that are extensively used. These methods have been employed concurrently [18] demonstrating good agreement on fatigue failure. Recorded measurements from these three methods appear to increase drastically in value at the failure point.

Numerical tools simulate the state of a component, including the stress distribution and magnitudes of stresses on the component under the applied condition. Its use is advantageous in analysing complex problems. Fatigue performance of components are extensively been evaluated with numerical tools [20-25]. Published literature has highlighted the importance of mesh refinement in critical areas such as the contact region [20] and stress concentration [21,22] to produce a more precise outcome when utilising numerical tools. Stress-life fatigue analysis utilised in the numerical tools adopts the local stress concept in evaluating fatigue. The hypothesis of the local stress concept in defining the fatigue performance is that if local stresses at critical locations of the component are known, the crack-initiation life of the component can be related to the empirical data [26].

Scarcity of experimental results and lack of public domain data on recycled rail is the driver for this investigation to identify the fatigue performance of recycled rail. Outcomes of this investigation will provide a better understanding of the reliability of recycled rail. It is essential to ensure the reliability of the recycled rail so that the implementation of recycling of rail can be carried out with confidence. Fatigue testing of high strength material is time consuming and requires advanced testing instruments with higher loading capabilities [13] to initiate cracks/failure. To overcome these constraints in an effective and efficient way, the novel method combining numerical and practical experiments was proposed for investigating the single opposite U-notched recycled rail specimen fatigue performance under cyclic compressive loadings.

METHODOLOGY

The integrated experimental and numerical method was used to determine the fatigue performance of a recycled rail specimen at 5×10^6 and 28×10^6 cycles and its endurance limit. The overall procedure is showed in Figure 1. The endurance limit was defined at 1×10^7 cycles as in most conventional fatigue test.

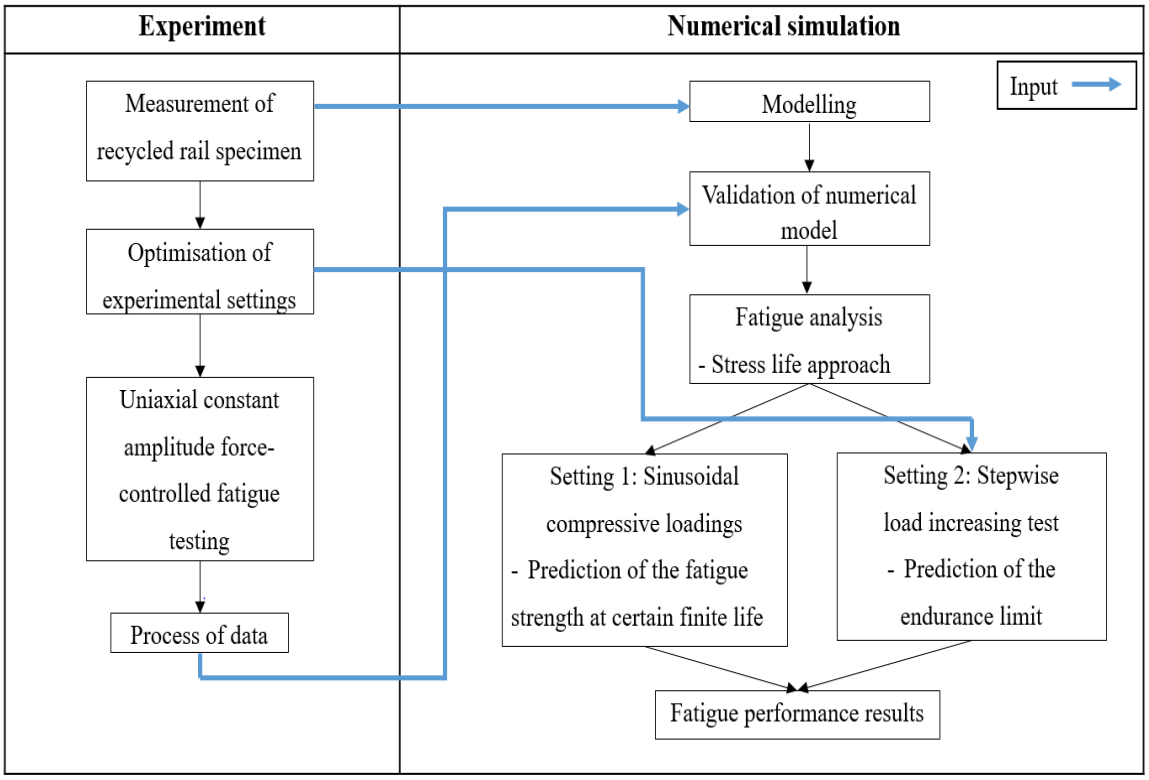

Figure 1. Procedure for fatigue strength and endurance limit determination by the integrated method.

Specimen material properties

The precise steel type for the specimen is unknown. According to published literature [27], in the early years, pearlitic carbon steels were the preferred steel for rail tracks. Properties and composition of rail steel are compelled to conform to the standard detailed in BS EN 13674-1:2011 [4]. For the purpose of this investigation, the rail specimen was assumed to be a medium carbon content non-alloy pearlitic steel as reported [20] to be used in the railway industry. Table 1 displays the mechanical properties for the assumed recycled rail specimen in this investigation.

Table 1. Rail steel mechanical properties [20].

Properties	**Value**
Cyclic strength coefficient, K' (MPa)	1523
Cyclic strain hardening, n'	0.19
A5 Elongation at Fracture (%)	19
Fatigue Strength Coefficient, σ'_f (MPa)	987
Fatigue Strength Exponent, b	-0.08
Fatigue Ductility Coefficient, ε'_f	0.106
Fatigue Ductility Exponent, c	-0.44
Tensile Strength, S_u (MPa)	790
Yield Stress, S_y (MPa)	455
Elastic Modulus, E (GPa)	210
Poisson's Ratio, ν	0.3

For the purpose of this investigation, the author was provided with a rectangular single opposite U-shaped notch recycled rail test specimen. The dimensions of this specimen is shown in Figure 2.

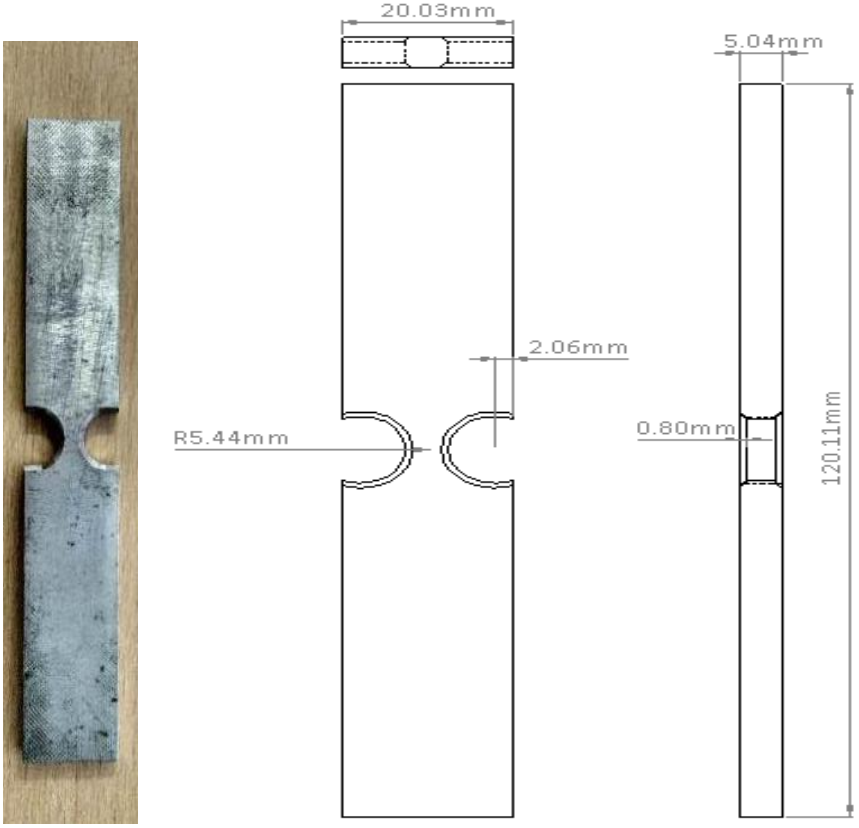

Figure 2. Test specimen with dimensions.

Experimental Method

The Instron E3000 fatigue machine was used to perform the uniaxial constant amplitude force-controlled fatigue test. This machine had a dynamic linear load capacity of 3000N with a nominal maximum capability of 100 Hz operating frequency. A number of test runs were conducted on this machine to determine a suitable operation rate. A 2000N compressive load at 50Hz operating frequency was determined as the machine optimal setting. An increase in load and frequency above the optimal setting caused the specimen to dislodge itself from the jaws of the machine. This issue could be attributed to the test characteristics and the shape of the jaws. Utilised load steps with the experimental settings are displayed in Table 2 and Figure 3.

Table 2. Fatigue experiment settings.

Parameters	Value
Frequency (Hz)	50
Maximum load (N)	0
Minimum load (N)	-2000
Mean load (N)	-1000

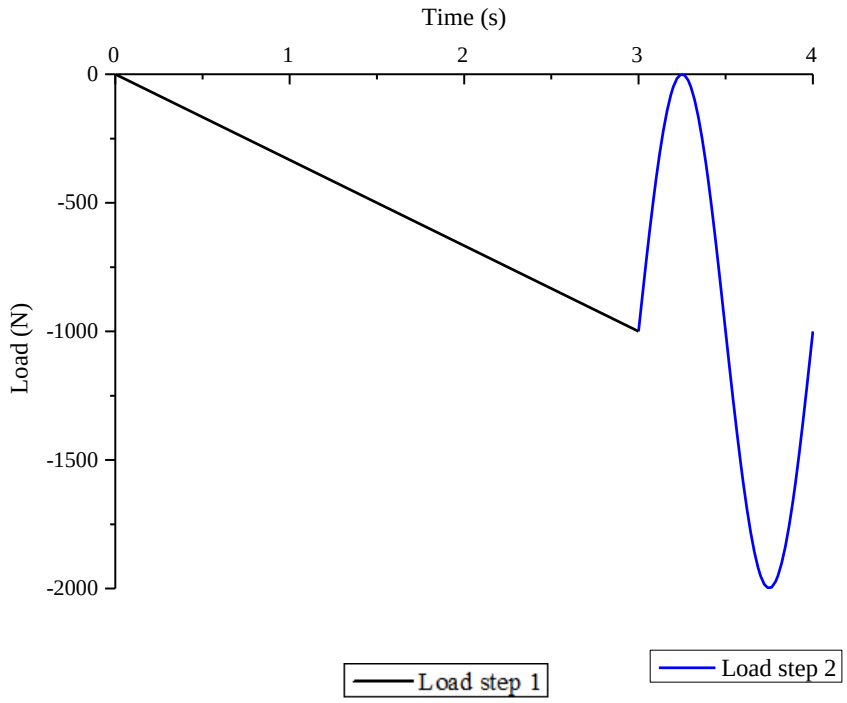

Figure 3. Experimental load steps (not to scale).

A total of 28,657,876 cycles was achieved after the specimen was tested over several separated days. Cycle time, load and displacement data were captured at 5,005,231 cycles and 28,657,876 cycles (quoted as 5 million cycles and 28 million cycles respectively in the

remaining of the paper). The nominal stresses at the critical area (the notch) were determined by dividing the measured applied loads by the net cross sectional area. The notch fatigue corrector (K_t = 1.28) which was derived from the size of the specimen and the dimensions of the U-shaped notch were also applied.

The material's endurance limit was determined using the stepwise (LIT) method because the author was only provided with one specimen. The constraints of this experimental test were the Instron E3000 fatigue machine loading capacity and the grip on its jaws. Therefore, to overcome this constraint, and as an alternative to conducting the stepwise load increase test experimentally, a numerical tool was employed to simulate this stepwise load increase test.

Numerical Method

ANSYS workbench was used to carry out the stepwise load increase test. Figure 4 illustrates the U-notched recycled rail specimen model, boundary conditions and mesh. The model consisted of 4513 elements and 7398 nodes. Reflecting the experimental setup on the fatigue machine, an oscillating load was employed normal to the area on top of the specimen with the specimen base fixed supported.

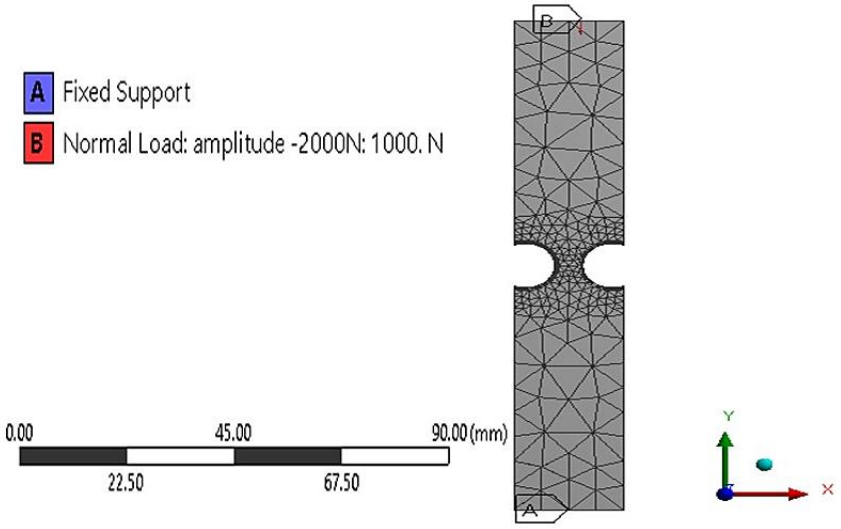

Figure 4. The boundary conditions and mesh refinement around the notch of the recycled rail specimen.

The mesh of the specimen was made up of SOLID187 [28] (quadratic 10-nodes element) for the main body and SURF154 [28] at the load surface. A suitable mesh density and hardware processing period was determined from the performed mesh convergence study. Following this, a coarse mesh including a slow transition and level 1 refinement for the 6 faces at both notches giving the highest average mesh aspect ratio (i.e. least distorted meshed element shape) — 0.7172 with the least deviation from experimental result was identified as the definitive mesh setting. To achieve a valid numerical approach using the Finite Element (FE) prediction model, results of the FE analysis and the experimental approach were compared. When the 2000N load was applied, the maximum compressive stress on the FE model was 106.23MPa whilst the median value measured from the

experiment was 96.85MPa. Both experimental and FE results were plotted as shown in Figure 5. An approximate difference of 9.7% was recorded. A gross stress of 19 MPa was obtained by dividing the load by the total of the specimen's width multiplied by its thickness. The results from the experiments were in good agreement with the gross stress values of 16 – 20MPa generated by the FE model. The FE model also demonstrated that the compressive stresses converged at the neck of the specimen. This conforms to the theoretical assumption which validates the model.

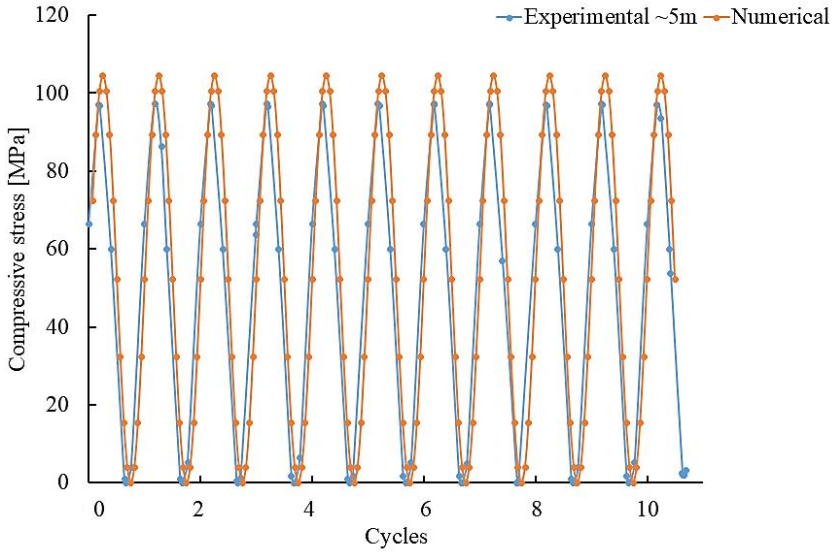

Figure 5. Comparison between the numerical model and experimental result for model validation.

Equivalent stress (von Mises stress) criterion that considers multiaxial stresses at the critical location and suits ductile material was used for the stress-life fatigue analysis. As the best predictor of failure for the ductile material validated by experimental observation, the Gerber theory was used to determine the mean stress correction [29]. The dimensions of the U-shaped notch, fatigue strength factor, K_f = 0.72 (established from the specimen size) and additional factors such as those shown in Table 3 were used to determine the notch stress concentration. The component is considered to have failed when the computed fatigue result indicates a safety factor below 1 or fatigue damaged is greater than 1.

Table 3. Fatigue modification factors.

Modification factor	**Value**	**Note**
Fatigue stress concentration – Notch, k_f	0.80	[26,30]
Size, k_{sz}	0.90	
Surface condition, k_{sr}	1.00	Polished specimen
Temperature, k_T	1.00	k_T=1.0 when the temperature ≤ 450^o
Load, k_L	1.00	k_L= 1.0 for Axial loading

Figure 6 shows an applied compressive sinewave load of 50 Hz to determine the specimen's fatigue strength at 5 million and 28 million cycles. The load amplitude was added in increments of 100N till the fatigue safety factor value of 1 was reached. At this point the load increments were altered to ± 50N to help approximate the failure load.

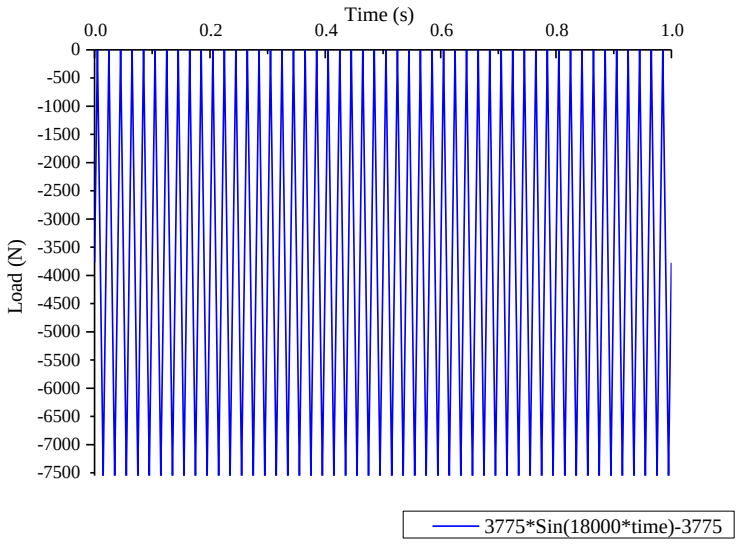

Figure 6. Compressive cyclic loading on the specimen for 5 million cycles.

Next, the stepwise load increase test method was applied in the FE model to determine the endurance limit. Figure 7 and Table 4 shows the setup of the stepwise load increase test (LIT) test. The 2000 N experimental load and 50Hz frequency was the adopted lower load limit value. An increment of 250N was applied at each interval of 5×10^6 cycles. The loadings in the stepwise LIT method was a non-constant amplitude loading. The definition of fatigue life is the quantity of loading blocks till failure for the non-constant loading fatigue analysis. Therefore in this situation, the total load step is identified as a loading block. In order to reduce the numerical computation time, the simulation was scaled down by a factor of 100000 and each load step was run for 1s (50 cycles) until failure to pinpoint the failure load step. Direct scaling of the numerical result was carried out to determine the estimated fatigue life for the actual condition (5×10^6 cycles per load step). In estimating the fatigue strength, the similar scaling concept was adopted for the 5 million and 28 million cycles.

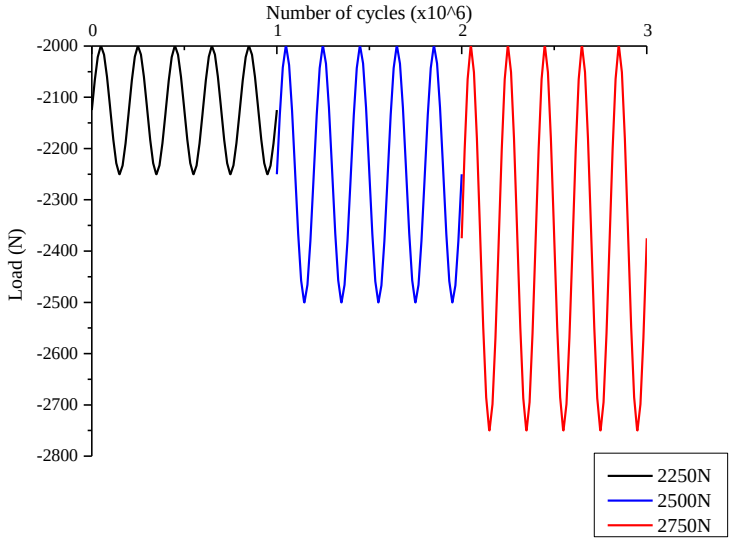

Figure 7. Stepwise load increase test loadings (not to scale, frequency = 50 Hz).

Table 4. Stepwise LIT method fatigue test parameters in compression load.

Load step	Minimum force, F_{min} (N)	Maximum force, F_{max} (N)	Mean load, F_m (N)	Amplitude, A (N)	Accumulated number of cycles, N ($\times 10^6$)
1	2000	2250	2125	125	5
2	2000	2500	2250	250	10
⋮	⋮	⋮	⋮	⋮	⋮
n	2000	2000 + 250n	$\frac{F_{max}+F_{min}}{2}$	$\frac{F_{max}-F_{min}}{2}$	5n

RESULTS AND DISCUSSION

The fatigue characteristics – the fatigue strength and endurance limit and reliability of recycled rail not publicly available were determined by the novel integrated experimental and numerical method.

It has been noted that the difference in the stress and strain values at 5 million and 28 million cycles are negligible as seen from the outcome of the experimental fatigue test. The values of 96.85 MPa and 0.00085 mm/mm were the median peak compressive stress and strain respectively at 5 million cycles. Values rose marginally to 97.04 MPa and 0.00088 mm/mm respectively for the 28 million cycles. Figure 8 showed the comparison of the average peak compressive stresses for both the 5 million and 28 million cycle experiments over 10 cycles.

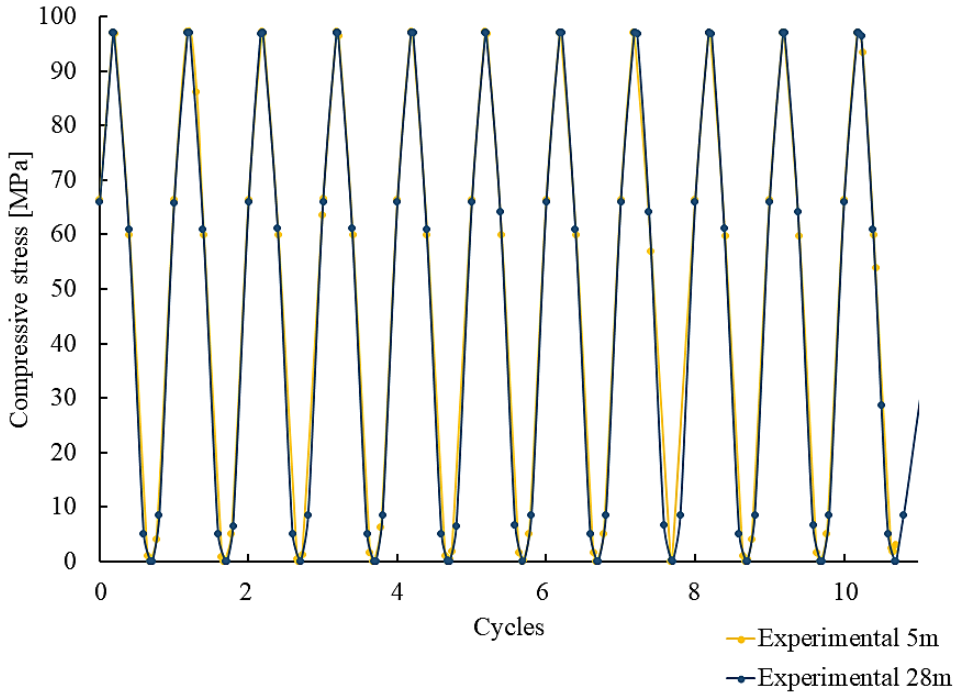

Figure 8. Comparison of average peak compressive stresses between 5 million and 28 million cycles fatigue test.

There were no dimensional changes measured in the test specimen after being subjected to a fatigue test of 28 million cycles. Theoretically the specimen must undergo a permanent change in dimension when it is fatigue damaged. The specimen reverted to its initial size even though there was an increase in strain values at higher cycles. As no fatigue failure occurred during the tests this intimated that applied load was too small to have a major impact. Therefore, this meant that even at high cycles the scale of the developed compressive stresses due to the applied load was unable to provide a notable impact. Despite the preventive measures taken to consistently position the specimen in the jaws of the fatigue machine, small discrepancies in stress-strain values between the 5 and 28 million cycles fatigue tests were noticed. This could be due to the modest change in the alignment of the specimen within the jaws of the machine. This issue transpired whenever the specimen was removed and repositioned back into the jaws.

The numerical method showed that the 7550N (Figure 9) and 5300N (Figure 10) compressive loads caused the specimen failure at 5 million and 28 million cycles respectively. It was predicted to fail at 4.9094×10^{6} cycles at the applied load of 7550N. 138.86 MPa was the fatigue strength of the specimen which is also recognised as the maximum equivalent alternating compressive stress under the 7550N load. For the applied load of 5300N it was predicted to fail at 2.7215×10^{7} cycles. 96.707MPa was the maximum induced equivalent alternating compressive stress. When the designed service life of the specimen was extended, a significant reduction was noticed in the alternating stress that could be endured by the specimen.

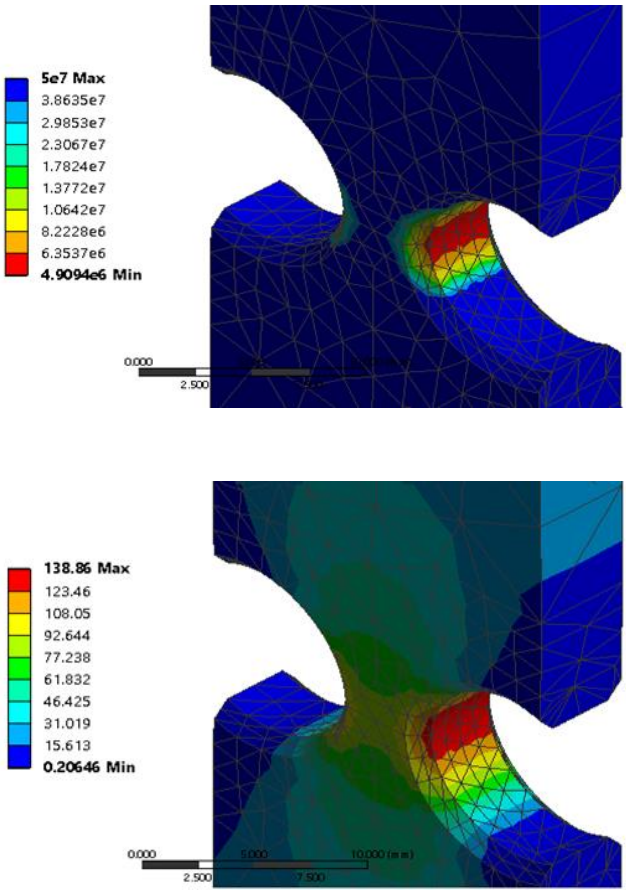

Figure 9. Fatigue life (top) and equivalent alternating stress distribution (bottom) under the 7550N load.

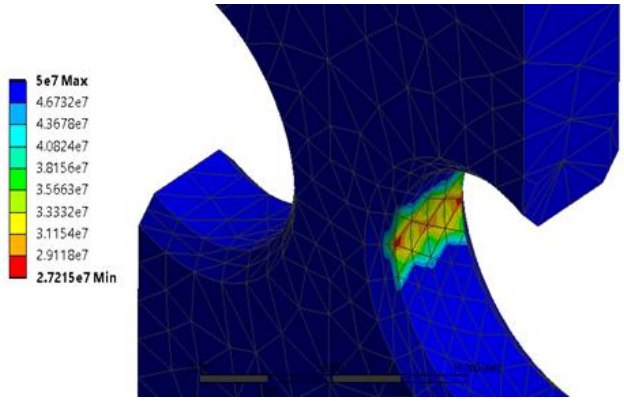

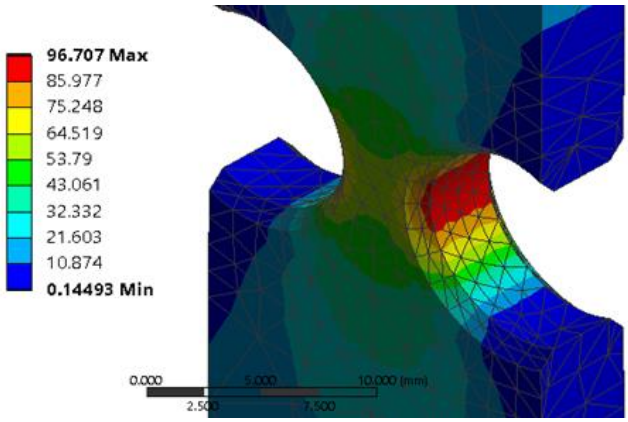

Figure 10. Fatigue life (top) and equivalent stress distribution (bottom) under the 5300N load.

From the stepwise LIT method, the failure load for the specimen was 2500N. The specimen failed when the safety factor for the designed life (1×10^7) fell to 0.86023. The specimen was able to withstand the applied load up until 6.2202×10^6 cycles before failure. According to the stepwise LIT method, the estimated endurance limit is the stress amplitude of the load step that caused the failure [14]. Therefore, a stress amplitude value of 130.37MPa in the failure load step 2 was identified as the specimen's endurance limit value.

For the 5 million cycles, 28 million cycles and stepwise load increase test method cases, the root of the U notches was the critical area as shown in Figure 11. The recorded shortest fatigue life and the highest fatigue damage was at this critical location. Due to the nature of stress concentrations, the notch root is acknowledged as the prime area for fatigue failure. The presence of a notch in the specimen changes its cross-sectional area thereby increasing the stresses in the notch. This is comparable to the situation where a fluid flows through a restricted segment. Stresses have the tendency to advance into areas of low stress dependent on the geometry and mode of loading. Therefore, based on this understanding the location where the failure occurs first is the notch. As shown in Figure 12, the maximum stress values around the notch root increased from 117.4MPa to 130.4MPa as it proceeded to the next load step containing a higher load amplitude.

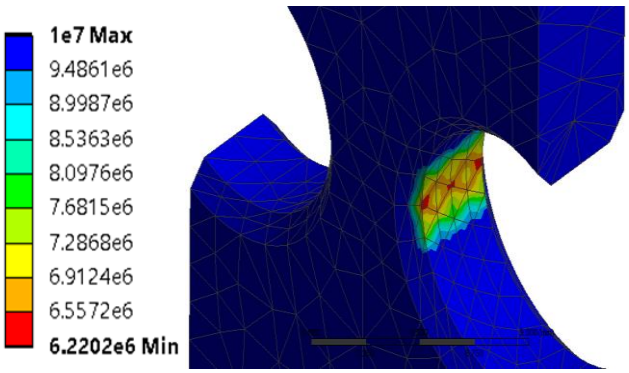

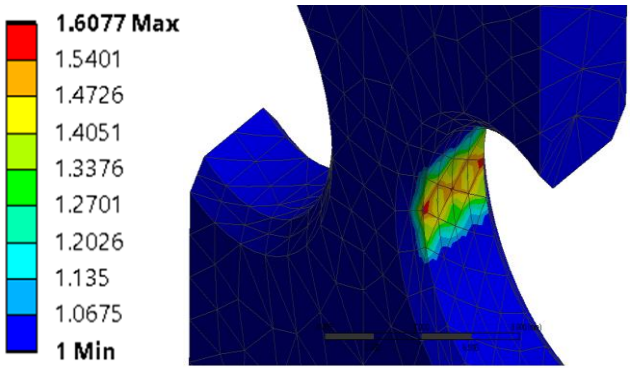

Figure 11. Fatigue life (top) and fatigue damage at notch root (bottom) in stepwise load increase test (LIT).

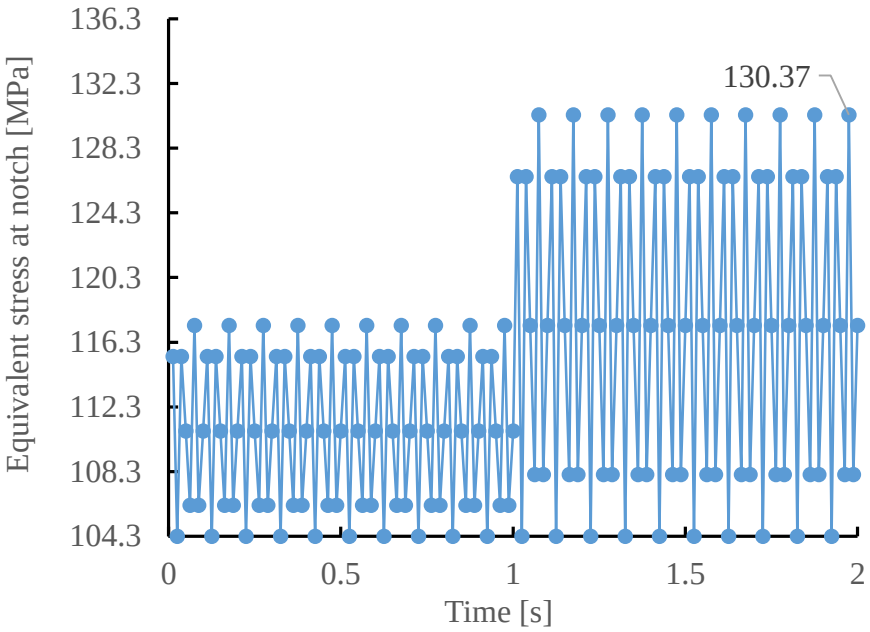

Figure 12. Variation of equivalent stress over load steps (1 s = 50 cycles = 1 load step in stepwise load increase test).

It has regularly been presumed that compressive loading does not influence crack development of a smooth (physically flawless) specimen as compared to a fully reversible or tension-tension loading. This statement however is incorrect if specimen geometrical discontinuities exist [31]. Figure 13 shows that the stresses at the opening of both notches are positive (tensile stresses) as observed by the stress distribution in the specimen. Throughout the unloading stage of the compression loading process, the residual tensile stresses are concentrated at the opening zones. The initiation of a crack under the compressive cyclic loading, is because of the residue tensile effect as the tensile stresses attempt to pull the specimen apart at the notch root [31]. When the cracks start at the root, its propagation is stimulated by the residual tensile stresses and stress gradient which ultimately causes specimen failure due to fatigue.

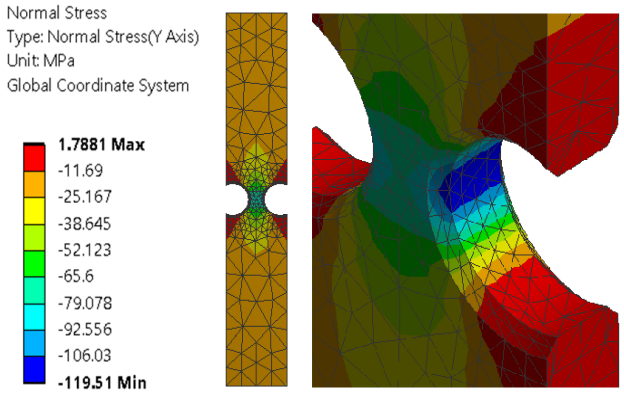

Figure 13. Front view (left) and enlarged, isometric view (right) of the Y-Axis normal stress distribution for the 2500N load in the stepwise load increase test (LIT) method.

The analytic results calculated using Equation (1) and the results of the integrated method were tabulated in Table 5. Generally, the outcomes were consistent because as the number of cycles increased, the fatigue strength of the specimen decreased. It is shown that the fatigue strength values obtained through the integrated method were lower than the analytical method. The percentage difference between the endurance limit of the integrated method and analytical method is 39%. In Figure 14, the results showed that the graphs for the integrated and analytical methods have the same trend but differ considerably in their quantified fatigue strength (as seen in Table 5). This demonstrated that the integrated method is a reliable method that can be utilised in place of the analytical method. Figure 14 also shows the reduction in fatigue stress amplitude from the 5 to 10 million cycles (reduction gradient, m = 1.7291) was 6% lower than that of the 10 to 28 million cycles (m = 1.8326).

Table 5. Summary of result.

	Integrated experimental and numerical method (MPa)	**Analytical method (MPa)**	**Percentage difference (%)**
Fatigue strength at 5 million cycles	138.86	210.56	41.04
Fatigue strength at 28 million cycles	96.71	170.79	55.38
Endurance limit (10 million cycles)	130.37	193.55	39.01

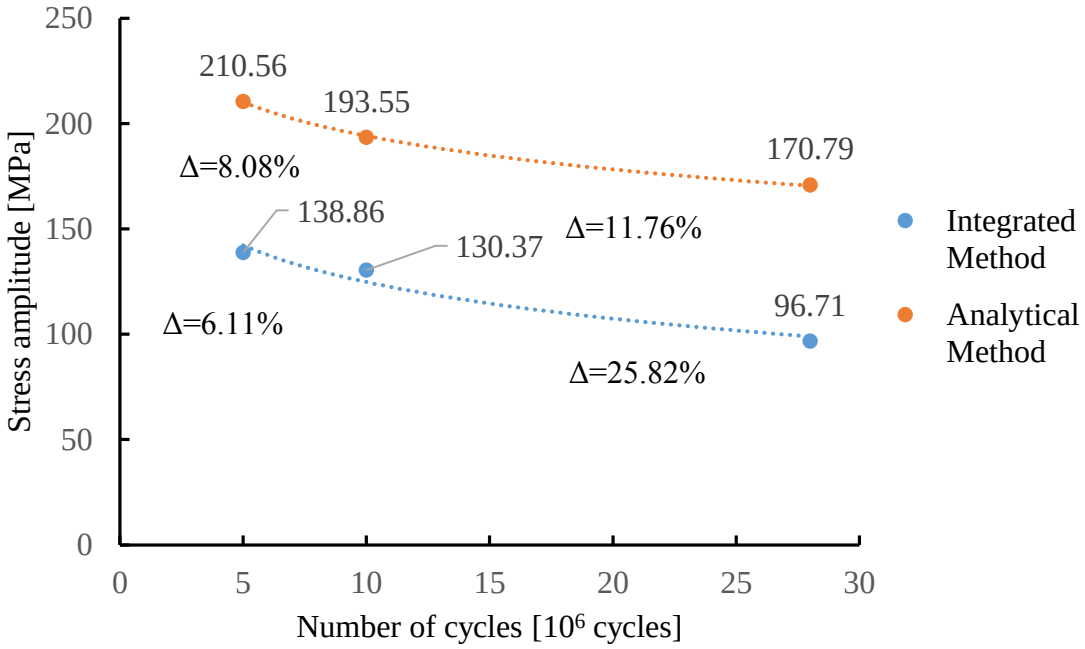

Figure 14. Graph of results from the integrated method and analytical method.

The integrated method also predicted a lower fatigue strength reduction (6.11%) between the 5 and 10 million cycles as compared to the result of the analytical method (8.08%). Then, the strength amplitude of the integrated method dropped significantly by 25.82% between the 10 and 28 million cycles while the reduction for the analytical method was 11.76%. The results of the integrated method observed a higher degree of fatigue resistance retention at lower cycle and a greater degree of reduction in fatigue resistance after the loss of residual stress stability at high cycle counts.

The shot blasting process induced the compressive residual stress thereby renewing the strength of the rail surface [8]. The phenomena helped stall the crack initiation effectively slowing down its propagation. This was vital in strengthening the fatigue resistance of the material. However, there is a limit to the improvement of the fatigue resistance because after repeated cycles, the compressive residual stress will relax. Hence, the stress amplitude can be supported by the component tends to reduce further with the loss of its compressive residual stress at high cycles. The integrated method was able to better capture this phenomenon of good fatigue resistance as demonstrated by the predicted reduction of 6.11% for the integrated method in comparison to a reduction of 8.08% for the analytical method. This result is also seen again in the deterioration due to the residual stress relaxation at high cycles where the integrated method reduced by 25.82% in comparison to a reduction of 11.76% for the analytical method. Hence, the result of the compressive residual stress affecting the fatigue strength of the recycled rail was more prominently reflected in the results from the integrated method than the analytical method. This reaffirms the argument that with the inclusion of the experimental data into the integrated method, the integrated method is a better predictor of the actual recycle rail fatigue strength as compared to the analytical method.

The recycled rail specimen has shown satisfactory fatigue performance. According to BS EN 13674-1:2011 [4], a successful rail steel specimen must withstand a fatigue test of more than 5×10^6 cycles for a total strain amplitude of 0.00135 mm/mm. As shown in Figure 15, the recycled rail specimen has over-performed because its maximum strain amplitude was 0.0018755 mm/mm before it failed at 5×10^6 cycles under a compressive cyclic load of 7550N. This suggested that the life cycle of the rail material was not significantly impaired after recycling. This demonstrates that the service life of the rail track can be extended by recycling it without compromising its performance. In addition to this, the original track operation and maintenance scheme as for the new rail could be directly implemented on the recycled rail, eliminating the need of setting up a special scheme for the recycled rail.

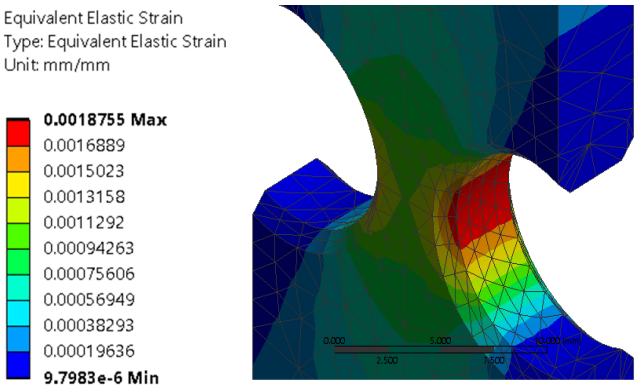

Figure 15. Strain amplitude of the specimen under 7550N.

CONCLUSIONS

A novel method of integrating experimental fatigue test results with finite element analysis (FEA) and stepwise load increase test (LIT) method was proposed to investigate the fatigue performance of a recycled rail specimen. The integrated method utilised conventional constant stress amplitude force controlled fatigue testing to provide important data for numerical modelling. The difference between the numerical model in the integrated method and the experimental fatigue testing results was less than 10%. The stepwise LIT technique was utilised in the numerical analysis. The stepwise LIT simulation was scaled down to reduce the numerical computation time.

A value of 130.37MPa was the estimated endurance limit of the recycled rail specimen. The novel integrated approach provided a more conservative prediction of fatigue performance (39% lower) than conventional analytical method. The integrated method was able to demonstrate the improved fatigue strength generated by shot blasting process and its deterioration caused by the relaxation of the residual stress at higher cycles. Besides, the specimen is capable to support a maximum of 0.0018755 mm/mm strain amplitude, higher than the required amplitude of 0.00135mm/mm at 5×10^6 cycles.

Fatigue testing of rail specimens is time consuming and requires a high capability fatigue machine due to the high resilience and quality of the rail steels used for large rail

track systems. With the integrated method, the cost in experimentation time and testing instrument to derive the fatigue properties of the high strength metals could be reduced effectively. Due to the limited availability of published recycled rail fatigue performance data, outputs derived from this proposed integrated method provide invaluable evidence to demonstrate that it is safe to use recycled rail. This therefore increases the confidence level of the safety integrity of recycled rail.

Going forward it would be beneficial if further experimental work is conducted to validate the accuracy of the direct conversion of the scaled down numerical stepwise load increase test result. This additional information would be of great benefit to both academia and industry as it would further substantiate the findings of this investigation

REFERENCES

[1] Worldsteel Assosiation. High-speed rail networks: A sustainable steel solution. 2015.
[2] Taylor G. Lengthy Recycling. The Rail Engineer. 2012; 91: 38.
[3] Network Rail Media Centre. Rail recycling depot to save network rail £4M a year. 2012.
[4] British Standards Institution. BS EN13674-1:2011 Railway applications - Track – Rail Part 1: Vignole railway rails 46 kg/m and above. BSI, London. 2011.
[5] Ekberg A, Åkesson B, Kabo E. Wheel/rail rolling contact fatigue – Probe, predict, prevent. Wear. 2014; 314: 2–12.
[6] Nouguier-Lehon C, Zarwel M, Diviani C, Hertz D, Zahouani H, Hoc T. Surface impact analysis in shot peening process. Wear. 2013; 302: 1058-1063.
[7] Benedetti M, Fontanari V, Winiarski B, et al. Fatigue behaviour of shot peened notched specimens: effect of the residual stress field ahead of the notch root. Procedia Engingeering. 2015;109:80–88.
[8] Dalaei K, Karlsson B, Svensson L-E. Stability of shot peening induced residual stresses and their influence on fatigue lifetime. Materials Science and Engineering. 2011; A528:1008–1015.
[9] Dalaei K, Karlsson B, Svensson L-E. Stability of residual stresses created by shot peening of pearlitic steel and their influence on fatigue behaviour. Procedia Engineering. 2010; 2:613–622.
[10] Dalaei K, Karlsson B. Influence of shot peening on fatigue durability of normalized steel subjected to variable amplitude loading. International Journal of Fatigue. 2012;38:75–83.
[11] Kim J, Cheong S, Nogichi H. Residual stress relaxation and low- and high-cycle fatigue behaviour of shot-peened medium-carbon steel. International Journal of Fatigue. 2013;56:114–122.
[12] Azar V, Hashemi B, Yazdi MR. The effect of shot peening on fatigue and corrosion behaviour of 316L stainless steel in Ringer's solution. Surface & Coatings Technology. 2012;204:3546–3551.
[13] Hansson T. Fatigue failure mechanisms and fatigue testing. NATO Science and Technology Organisation, Educational Notes RDP, RTO-EN-AVT-207-14. 2012; 1–23.

[14] Casado JA, Carrascal I, Polanco JA, et al. Fatigue failure of short glass fibre reinforced PA 6.6 structural pieces for railway track fasteners. Engineering Failure Analysis. 2016;13:182–197.
[15] Thomas C, Sosa I, Setien J, et al. Evaluation of the fatigue behaviour of recycled aggregate concrete. Journal of Cleaner Production. 2014;65:397–405.
[16] Starke P, Walther F, Eifler D. 'PHYBAL' a short-time procedure for a reliable fatigue life calculation. Advanced Engineering Materials. 2012;12(4):276–282.
[17] Kucharczyk P, Rizos A, Munstermann S, et al. Estimation of the endurance fatigue limit for structural steel in load increasing tests at low temperature. Fatigue Fatigue and Fracture of Engineering Materials and Structure. 2012;35:628–637.
[18] Imran M, Siddique S, Guchinsky R, et al. Comparison of fatigue life assessment by analytical, experimental and damage accumulation modelling approach of steel SAE 1045. Fatigue and Fracture of Engineering Materials and Structure. 2016;39:1138–1149.
[19] Nicholas T. Step loading for very high cycle fatigue. Fatigue and Fracture of Engineering Materials and Structure. 2002;25:861–869.
[20] Reis L, Li B, de Freitas M. A multiaxial fatigue approach to Rolling Contact Fatigue in railways. International Journal of Fatigue. 2014;67:191–202.
[21] Guechichia H, Benkabouchea S, Amroucheb A, et al. A high fatigue life prediction methodology under constant amplitude multiaxial proportional loadings. Materials Science and Engineering. 2011; A528:4789–4798.
[22] Słowik J, Łagoda T. The fatigue life estimation of elements with circumferential notch under uniaxial state of loading. International Journal of Fatigue. 2011;33:1304–1312.
[23] Yunoh MFM, Abdullah S, Saad MHM, Nopiah ZM, Nuawi MZ. Fatigue feature extraction analysis based on a K-Means clustering approach. Journal of Mechanical Engineering and Sciences. 2015;8:1275-82.
[24] Mohamed MA, Manurung YHP, Ghazali FA, Karim AA. Finite element-based fatigue life prediction of a load-carrying cruciform joint. Journal of Mechanical Engineering and Sciences. 2015;8:1414-25.
[25] Fauzun F, Aqida SN, Naher S, Brabazon D, Calosso F, Rosso M. Effects of Thermal Fatigue on Laser Modified H13 Die Steel. Journal of Mechanical Engineering and Sciences. 2014;6:975-80.
[26] Darrell FS. Fatigue-life Prediction Using Local Stress-Strain Concepts. Experimental mechanics. 1977;17(2):50–56.
[27] Yates JK. Innovation in Rail Steel. Science in Parliament. 1996;53:2–3.
[28] ANSYS, Inc. ANSYS mechanical APDL element reference. ANSYS Release 15.0 SAS IP, Inc. 2013.
[29] Schmid SR, Hamrock BJ, Jacobson BO. Fundamentals of Machine Elements. Boca Raton: CRC Press. 2014.
[30] Warren CY, Richard GB. Chapter 17 Stress concentration. Roark's formulas for stress and strain. New York: McGraw-Hill. 2002; 771–796.
[31] Hsu T, Wang Z. Fatigue crack initiation at notch root under compressive cyclic loading. Procedia Engineering. 2010;2(1):91–100.